



# Comparison of Spectralis and Cirrus spectral domain optical coherence tomography for the objective morphometric assessment of the neuroretinal rim width

Christoph Mitsch<sup>1</sup> · Stephan Holzer<sup>1</sup> · Lorenz Wassermann<sup>1</sup> · Hemma Resch<sup>1</sup> · Susanne Urach<sup>2</sup> · Barbara Kiss<sup>1</sup> · Anton Hommer<sup>3</sup> · Clemens Vass<sup>1</sup>  · Ursula Schmidt-Erfurth<sup>1</sup>

Received: 14 January 2019 / Revised: 4 March 2019 / Accepted: 15 March 2019 / Published online: 29 March 2019

© The Author(s) 2019

## Abstract

**Purpose** The assessment of cup-disc ratio as a surrogate parameter for the neuroretinal rim width (NRW) of the optic nerve is well established, but prone to human error and imprecision. Objective assessment of the NRW is provided by spectral domain optical coherence tomography (SD-OCT). This study is the first to systematically compare NRW measurements acquired with the Carl Zeiss Meditech Cirrus HD-OCT 5000 and the Heidelberg Engineering Spectralis SD-OCT.

**Methods** In this cross-sectional study, 20 eyes of each 20 glaucoma patients and 20 age-matched healthy controls underwent ophthalmic examination, SD-OCT imaging, and computer perimetry. Regression analyses were performed for the NRW comparability and the effect of the rotational alignment discordance (RAD), receiver-operating characteristics (ROC) for NRW-based healthy glaucoma discrimination capability, and Pearson's correlation for covariate association.

**Results** Mean NRW differences were  $8 \pm 48 \mu\text{m}$  ( $p = 0.4528$ ),  $91 \pm 80 \mu\text{m}$  ( $p < 0.01$ ), and  $49 \pm 77 \mu\text{m}$  ( $p < 0.001$ ) in the glaucoma, healthy, and whole group. On average, the Cirrus showed higher NRW values (+ 50  $\mu\text{m}$ ) than the Spectralis, this difference increased with values starting with 159  $\mu\text{m}$ . Discrimination ROC were 1.0 (Spectralis) and 0.9675 (Cirrus). RAD showed very little effect on NRW ( $R^2 = 0.9661$ ,  $p < 0.001$ ). NRW-covariate correlation was highly significant ( $p < 0.001$ ) with both devices for clinical cup/disc ratio, calculated rim width, visual field mean, and pattern deviations.

**Conclusions** Our results suggest to only cautiously compare Spectralis and Cirrus NRW measurements only in patients with morphologically manifest glaucoma. For morphological progression analysis, we recommend the continuous usage of the same device.

**Keywords** Glaucoma · Optic disc · Optical coherence tomography · Neuroretinal rim width

## Introduction

Glaucoma is defined as an optic neuropathy with progressive loss of retinal ganglion cells and associated morphological

changes to the optic nerve and retinal nerve fiber layer (RNFL), respectively [1]. Loss of visual function in glaucoma is generally irreversible and, without adequate treatment, the disease can lead to visual impairment or blindness [1]. Morphological damage may precede a loss of function by many years, and precise imaging techniques are fundamental for a detection of progression, especially at earlier stages of damage [2]. Next to assessing the visual field, diagnosis and management of glaucoma are based on the detection of morphometric changes to the optic nerve head (ONH) and peripapillary RNFL for years in the progress of the disease. Using spectral domain optical coherence tomography (SD-OCT), the configuration of the ONH and the thickness of the peripapillary RNFL can be objectively measured [3]. Change over time in RNFL thickness, measured with a circular peripapillary SD-OCT scan pattern, is widely accepted as a marker for progression of glaucomatous optic neuropathy. Still, it is limited by imaging artifacts, which

---

**Electronic supplementary material** The online version of this article (<https://doi.org/10.1007/s00417-019-04299-x>) contains supplementary material, which is available to authorized users.

---

✉ Clemens Vass  
clemens.vass@meduniwien.ac.at

<sup>1</sup> Department of Ophthalmology and Optometry, Medical University of Vienna, Waehringer Guertel 18-20, 1090 Vienna, Austria

<sup>2</sup> Center for Medical Statistics, Informatics and Intelligent Systems, Medical University of Vienna, Vienna, Austria

<sup>3</sup> Hommer Ophthalmology Institute, Albertgasse 39, Vienna, Austria

influence the correct segmentation of the RNFL and may to some extent be consequences of decreased OCT reflectivity in glaucoma [4]. Recently, another anatomic SD-OCT biomarker describing the neuroretinal rim anatomy gained clinical importance and in some studies proved to surpass other parameters in the diagnostic power for glaucoma [5–10]. Two widely used SD-OCT devices, the Spectralis® spectral domain optical coherence tomograph (Heidelberg Engineering GmbH, Heidelberg, Germany) and the Cirrus® high-definition optical coherence tomograph (Carl Zeiss Meditech Inc., Dublin, CA, USA) offer the possibility of quantifying the neuroretinal rim width (NRW). Having introduced those measurements into our clinical practice some years ago, we learned that the reports of the Cirrus OCT (which include exemplary b-scans showing the limits of the NRW measurements) did not correspond in detail with Spectralis OCT assuming the same segmentation and algorithm for measuring the NRW. We recognized that the ILM-sided limits of the vector connecting the ILM and the Bruch's membrane opening (BMO) of the Cirrus OCT often were at different locations than those of the Spectralis OCT and apparently not at the ILM intersection the Spectralis OCT algorithm would have provided. Upon investigating, Carl Zeiss Meditec USA provided us with a US patent paper which, among other aspects, explains the algorithm used by the Cirrus OCT for the determination of the NRW [11]. Cirrus NRW is not optimized for the smallest distance, but for the smallest cross-sectional area of the RNFL at the optic disc. Refer to the “Methods” section of this article for details. Thus, concerning the Cirrus OCT and the Spectralis OCT, we are confronted with two rather different algorithmic approaches to determining the NRW.

To our knowledge, at present time, no study focused on comparing NRW measurements taken with those two devices. Hence, the aim of this study was to assess the comparability of NRW measurements of the Cirrus OCT and the Spectralis OCT.

## Methods

### Endpoints

1. Comparability of Spectralis OCT and Cirrus OCT NRW measurements, possibility of inferring a regression model equation for converting measurements of one device into values of the other and vice versa.
2. Discrimination capability of both devices between eyes with glaucoma and healthy eyes.
3. Quantification of the effect of the rotational alignment discordance (Cirrus OCT's acquired image frame vs. Spectralis OCT's anatomic landmark (BMO center—fovea plane) adjustment) on the MRW measurements. Description of this effect's consequences on the results of these analyses.

4. Association of the following covariates with the primary measurement values: best-corrected visual acuity (BCVA), axial eye length (AEL), intraocular pressure (IOP), cup-disc ratio (CDR), and optic disc diameter (ODD) as determined during slit-lamp examination, calculated rim width (CRW, calculated using the two former parameters, see “Methods” section), visual field mean deviation (MD), visual field pattern standard deviation (PSD), and RNFL thickness.

### Study setting

This cross-sectional study was performed at the Glaucoma Outpatient Clinic of the Medical University of Vienna's Department of Ophthalmology and Optometry. The study protocol was approved by the Ethics Committee of the Medical University of Vienna and followed the guidelines of Good Clinical Practice and the Declaration of Helsinki. The nature of the study was explained, and written informed consent was obtained for all subjects included.

### Study subjects

Inclusion criteria for primary open angle glaucoma (POAG) patients were suspect appearance of the ONH of at least one eye (either large cupping  $> 0.5$ , or asymmetry of cupping  $> 0.2$ , or localized rim loss, or failure of ISNT rule, or barring of circumferential vessels) and reproducible pathologic visual fields (VF) in standard automated perimetry (SAP) (either pathologic glaucoma hemifield test, or a cluster of 3 points in pattern deviation plot significant at 0.5% not located at the border of the VF). The VF defect had to be compatible with glaucoma and specifically with the appearance of the optic disc, and the mean defect (MD) had to be between  $-6$  and  $-15$  dB. For the group of healthy controls, subjects were included if slit lamp examination, indirect ophthalmoscopy, and computer perimetry results were normal, and IOP was less than 21 mmHg. If both eyes qualified for study, one was chosen at random.

Exclusion criteria included astigmatism greater than 2 diopters, myopia or hyperopia higher than 5 diopters, history of retinal pathologies, ocular trauma, acute angle closure or shallow anterior chamber angle, ocular inflammation or infection during the last 3 months, and ocular surgery or argon laser trabeculoplasty during the last 6 months.

### Clinical examination

During a single-day examination, each subject underwent the following clinical examinations: Slit lamp examination with ophthalmoscopy, during which the vertical optic disc diameter (ODD) was measured on a Haag-Streit 9000 slit lamp and a VOLK® Superfield® lens and denoted in millimeters (mm)

after correction for magnification dividing through 0.76. Also, the vertical CDR was assessed. Using ODD and CDR, the calculated rim width (CRW) was obtained mathematically:  $CRW = (1 - CDR) * ODD / 2$ .

Refractive error and best-corrected visual acuity (BCVA) were assessed using the ARK-1s auto-refractometer (NIDEK CO., LTD, Hiroishi Gamagori, Japan) and IOP with Goldmann tonometry. The AEL was measured in millimeters using the IOL-Master® 500 (Carl Zeiss Meditech Inc., Dublin, CA, USA). Visual field sensitivity was assessed using the Humphrey visual field analyzer (HFA; Carl Zeiss Meditech Inc., Dublin, CA, USA) and the full Swedish interactive threshold algorithm (SITA) 30-2 program.

## SD-OCT image acquisition and analysis

### Heidelberg Spectralis SD-OCT

SD-OCT measurement of the peripapillary RNFL as well as ONH parameters was performed using the Spectralis® -OCT Multicolor (Heidelberg Engineering, Heidelberg, Germany, software version 1.9.9.0). For technical details see Chauhan et al. 2013. In the Spectralis OCT, NRW is defined as the shortest distance between the BMO and the ILM. On each of the 48 radial scans centered on the optic nerve head, at rotational angular steps of 7.5° inter-scan angle (ISA), the BMO is two-dimensionally localized near the end of the highly reflective pigment epithelium. Simultaneously, the ILM is segmented and the shortest connection vector (SCV) between the BMO and the ILM along the scan is determined. The length of this SCV is returned as BMO-MRW. For each examination, fovea position and the automatic segmentation of Bruch's membrane and ILM were manually reviewed and confirmed at each radial scan for correctness following the procedure given by the device software.

### Zeiss cirrus HD-OCT

Cirrus OCT (Carl Zeiss Meditec, Dublin, CA, USA, software version 5.0.0.326) ONH measurements are based on volume scans consisting of 200\*200 A-scans manually centered on the ONH center. Radial scans at 2° ISA are interpolated. The rim area determination is based on a complex three-dimensional calculation taking the BMO as central margin, two adjacent scan axes as lateral edges, and the intersection of those radial scan axes with the ILM as the peripheral delimitations of trapezoidal polygons. The polygons are then optimized for minimum size. On each radial scan, a series of vectors starting at the BMO and ending at the intersection with the ILM is determined in their length. The angles of the vectors with the ONH plane resulting in the smallest area of the contained trapezoid (minimum rim area) are selected. The displayed NRW at each radial scan is the length of the

resulting lateral vectors containing each trapezoid. Refer to US patent US 20140081130 A1 for a detailed explanation of the algorithm and descriptive illustrations of the trapezoids' location [11]. After each examination, image quality and the automatic segmentation of Bruch's membrane and ILM were manually reviewed and confirmed at each reconstructed radial scan at angular intervals of 5°.

## Analysis

### Data preparation

Other than the Cirrus OCT, where the initially computed radial scan extends parallel to the horizontal acquired image frame (AIF) in temporal direction, the Heidelberg Spectralis acquires radial scans starting at the vector connecting the BMO center and the fovea (FoBMOC). Data were exported numerically using both manufacturers' export plugins. To achieve horizontal AIF rotational reference (=AIF corrected Spectralis), the native Spectralis NRW dataset was counter-rotated by the offset between the AIF and the FoBMOC. The Zeiss Cirrus was interpolated from originally 2° ISA to 7.5° ISA. This provided three datasets: Spectralis (native) NRW, Spectralis AIF NRW, and Cirrus NRW. Quadrants of the same arc length were calculated from values of the angle ranges  $[0^\circ - 45^\circ) + [315^\circ - 0^\circ)$ ,  $[45^\circ - 135^\circ)$ ,  $[135^\circ - 225^\circ)$ , and  $[225^\circ - 315^\circ)$  for the temporal, superior, nasal, and inferior quadrants, respectively. All data manipulation tasks were performed using MathWorks® MatLab™ R2016a and R version 3.4.3 (Kite-Eating Tree), released on 2017-11-30 [12].

### Statistical analysis

Although multiple tests were performed, no multiplicity correction was applied, because all analyses are considered exploratory. Results were considered significant at a level of  $p < 0.05$ .

### Comparability of Spectralis and Cirrus NRW measurements

The average of the subject mean NRW values in the different quadrants was compared between instruments, and the statistical significance of the differences was tested using a paired *t* test. Comparisons were also visualized in Bland-Altman plots. Additionally, box plots of the mean NRW in the four quadrants of healthy subjects and glaucoma patients were generated (see Fig. 1, lower line). For further illustration, the difference of the mean NRWs for healthy subjects and glaucoma patients was plotted along with their respective 95% confidence intervals (CI, see Fig. 3b). A regression model for both the mean NRW across all angles and also NRW at individual angles was calculated in order to estimate the measurements from one instrument based on results from the other.

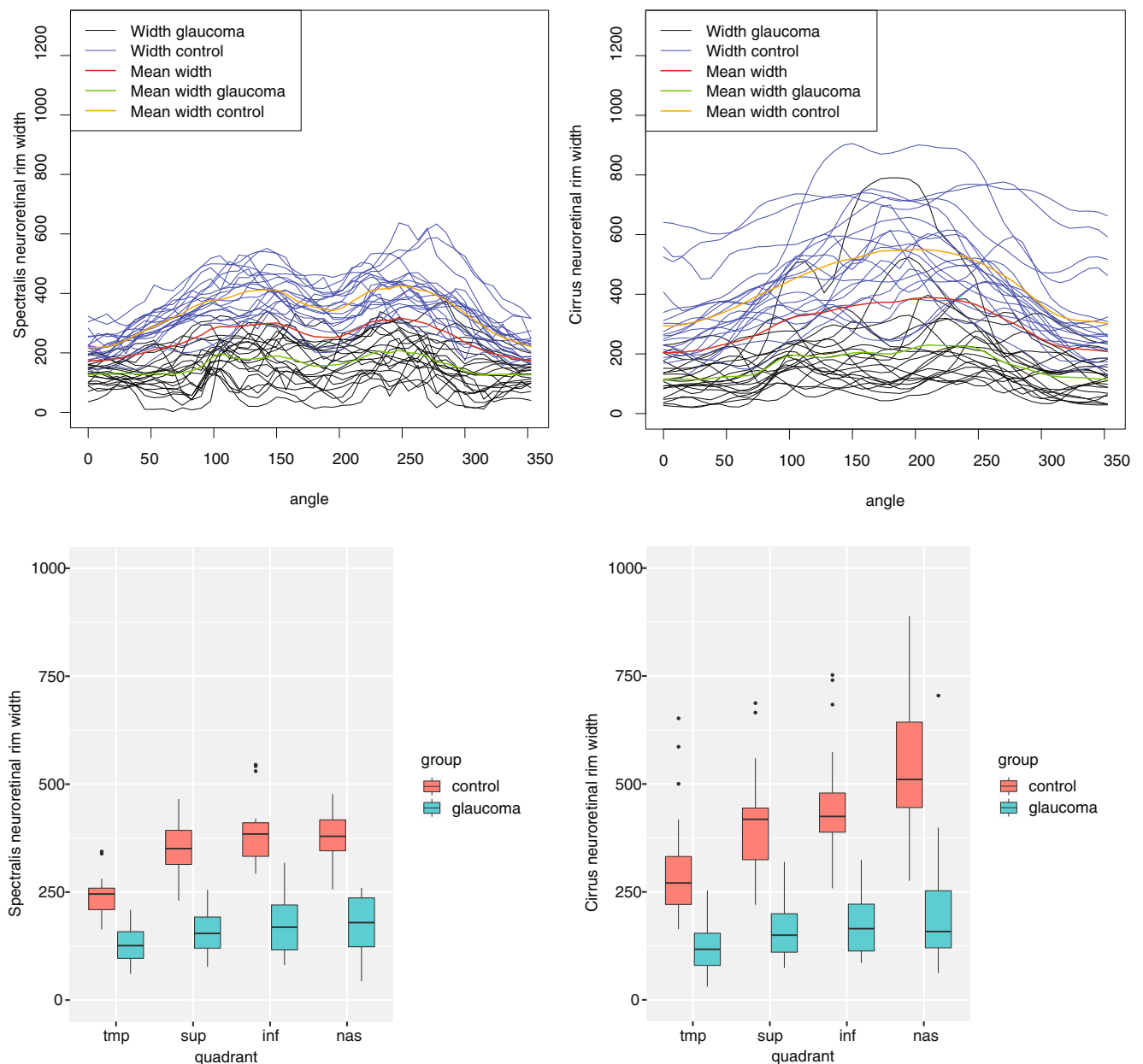


**Fig. 1** Upper line: Circumferential neuroretinal rim width trajectories of each patient with the Spectralis (upper left graph) and the Cirrus (upper right graph) OCT devices plotted along with the mean neuroretinal rim width trajectories for all subjects (red lines) and for the two groups of

glaucoma patients (green lines) and healthy subjects (orange lines). Lower line: Boxplots showing the Spectralis and Cirrus values in the four quadrants and in the glaucoma patients (green boxes) and healthy subjects (red boxes) group

**Discrimination capability between glaucoma patients and healthy subjects** Receiver operating characteristic (ROC) curves for the discrimination ability between the mean NRW values of glaucoma and healthy patients were plotted, and areas under the ROC curve (AUROC) were calculated.

**Effect of the rotational alignment discordance** A linear regression model for the effect of the rotational alignment difference of the native Spectralis and the AIF Spectralis dataset was generated.

**Association of covariates** To measure the association of the covariates BCVA, axial eye length, IOP, RNFL thickness, CDR, ODD, CRW, MD, PSD, and RNFL thickness with the mean NRW, the Pearson correlations together with the 95% CIs and *p* values were calculated.

## Results

Table 1 shows a summary of the baseline characteristics. We included 20 eyes of patients with glaucoma (mean age 71.18

**Table 1** Patient demographics

Characteristic	Glaucoma patients ( <i>n</i> = 20)	Healthy subjects ( <i>n</i> = 20)
Gender (f/m)	11 (55%)/9 (45%)	7 (35%)/13 (65%)
Age	71.18 ± 6.05 years	65.48 ± 8.13 years
Laterality (left/right)	12 (60%)/8 (40%)	11 (55%)/9 (45%)
Spherical refractive error	− 0.61 ± 2.16 D	− 0.28 ± 1.86 D
Cylindrical refractive error	0.89 ± 0.42 D	0.61 ± 0.50 D
BCVA	0.87 ± 0.18	0.93 ± 0.11
Axial eye length	23.93 ± 1.25 mm	23.67 ± 0.86 mm
Intraocular pressure	14.95 ± 3.03 mmHg	15.10 ± 2.49 mmHg
Cup/disc-ratio	0.84 ± 0.08	0.34 ± 0.13
Optic disc diameter	1.74 ± 0.15 mm (4 missing values)	1.71 ± 0.20 mm
Calculated rim width	0.15 ± 0.06 mm (4 missing values)	0.57 ± 0.12 mm
Visual field indices		
MD	− 10.24 ± 4.83 dB	− 0.63 ± 1.38 dB
PSD	11.07 ± 4.14 dB	2.01 ± 0.53 dB
Mean RNFL thickness		
Spectralis, mean	64.30 ± 14.84 μm	97.35 ± 7.96 μm
Cirrus, mean	68.22 ± 10.04 μm	91.89 ± 9.06 μm
Image quality		
Spectralis, dB	28.60 ± 2.44	30.25 ± 2.46
Cirrus, SNR	8.30 ± 0.92	8.75 ± 0.85

BCVA best-corrected visual acuity, given in Snellen; MD mean deviation on 30° SITA Humphrey computer perimetry; PSD pattern standard deviation on 30° SITA Humphrey computer perimetry; SNR signal/noise ratio

± 6.05 years), and 20 eyes of healthy subjects (age 65.48 ± 8.13 years). Image quality of OCT scans was within the range recommended by the manufacturers in all cases.

### Comparability of Spectralis and Cirrus NRW measurements

Table 2 shows the NRW measurements of the Spectralis OCT, the AIF-corrected Spectralis, and the Cirrus OCT.

NRW scattered markedly within each quadrant and extreme values were quite far from the mean. The empirical distributions of NRW in both subgroups were found to be approximately normally distributed for the Spectralis outcomes, but skewed or heavily tailed (containing outliers) for the Cirrus outcomes. This can also be observed on Fig. 1, the Cirrus measurements show more extreme values compared to the Spectralis measurements. Therefore, descriptive analyses were described not only by mean and standard deviation, but also by first quartile, median, and third quartile. Refer to Table 3 for a list of the differences between the measurements in all quadrants along with the Pearson correlation results and their significances.

For the whole cohort, mean NRWs measured with the Spectralis OCT were lower than those acquired with the Cirrus OCT (average global difference: − 49 μm), and all differences were statistically significant. In the glaucoma patient group, the mean global NRW difference between devices

was − 8 μm and not statistically significant ( $p = 0.4528$ ). In the healthy subject group, this difference was − 91 μm and statistically significant ( $p < 0.01$ ). Bland-Altman plots showed a dependence of the difference on mean NRW values (see Fig. 2). Spectralis NRW values were lower than Cirrus values above an average NRW value of 159 μm. The nasal quadrant displayed the largest difference between the devices with Spectralis NRW being 158 μm smaller than Cirrus NRW in healthy subjects. Figure 3a shows the mean NRW and Fig. 3b shows the mean NRW differences with values averaged over the 40 subjects for each measured angle.

### Regression model equation for calculating global Spectralis NRW values based on Cirrus measurements and vice versa

In Fig. 4, the global NRW of each subject measured with the Cirrus OCT is plotted against his global NRW with the Spectralis OCT. The linear regression of global Spectralis NRW values based on Cirrus measurements was  $y = -86 + 1.54x$  qualifying the increase in Cirrus global NRW ( $y$ ) with increasing Spectralis NRW ( $x$ ) with both intercept and slope being statistically significant ( $p < 0.001$ ). An increase in one unit of Spectralis mean NRW leads to an increase of 1.54 in Cirrus mean NRW. The linear regression of global Cirrus values based on Spectralis measurements was  $y = 75 + 0.58x$  qualifying the increase in Spectralis mean NRW ( $y$ ) with

**Table 2** Mean neuroretinal rim width in micrometers for the different quadrants

Group	Device/dataset	Value	Temporal ( $\mu\text{m}$ )	Superior ( $\mu\text{m}$ )	Nasal ( $\mu\text{m}$ )	Inferior ( $\mu\text{m}$ )
Overall	Spectralis	Mean $\pm$ SD	185 $\pm$ 72	252 $\pm$ 114	275 $\pm$ 122	285 $\pm$ 127
		Median, IQR	188 (129,245)	241 (158,351)	258 (180,378)	301 (169,384)
		Range	(61, 344)	(77, 466)	(44, 477)	(81, 545)
	Spectralis AIF	Mean $\pm$ SD	184 $\pm$ 71	260 $\pm$ 117	276 $\pm$ 121	277 $\pm$ 124
		Median, IQR	186 (125,246)	250 (158,364)	259 (185,380)	286 (168,374)
		Range	(59, 347)	(78, 477)	(45, 477)	(70, 545)
	Cirrus	Mean $\pm$ SD	213 $\pm$ 141	288 $\pm$ 163	372 $\pm$ 223	321 $\pm$ 177
		Median, IQR	190 (119,270)	260 (154,418)	320 (159,533)	318 (167,421)
		Range	(31, 652)	(74, 687)	(62, 889)	(85, 752)
Glaucoma Patients	Spectralis	Mean $\pm$ SD	128 $\pm$ 43	156 $\pm$ 56	172 $\pm$ 66	179 $\pm$ 64
		Median, IQR	126 (97, 158)	154 (120, 192)	179 (124, 237)	169 (116, 220)
		Range	(61, 209)	(3, 325)	(44, 260)	(81, 318)
	Spectralis AIF	Mean $\pm$ SD	128 $\pm$ 42	160 $\pm$ 58	173 $\pm$ 65	175 $\pm$ 65
		Median, IQR	122 (101, 155)	155 (119, 202)	183 (116, 238)	167 (117, 214)
		Range	(59, 209)	(78, 262)	(45, 261)	(70, 315)
	Cirrus	Mean $\pm$ SD	117 $\pm$ 59	160 $\pm$ 68	209 $\pm$ 144	183 $\pm$ 76
		Median, IQR	117 (80,154)	150 (110, 199)	158 (121, 253)	165 (113, 222)
		Range	(31, 253)	(74, 319)	(62, 705)	(85, 325)
Healthy Subjects	Spectralis	Mean $\pm$ SD	241 $\pm$ 46	349 $\pm$ 61	378 $\pm$ 62	390 $\pm$ 75
		Median, IQR	246 (209,259)	351 (314, 393)	379 (346, 417)	385 (333, 410)
		Range	(163, 344)	(231, 466)	(257, 477)	(293, 545)
	Spectralis AIF	Mean $\pm$ SD	240 $\pm$ 46	360 $\pm$ 61	378 $\pm$ 62	379 $\pm$ 75
		Median, IQR	246 (212, 259)	366 (320, 404)	382 (344, 419)	375 (327, 395)
		Range	(159, 347)	(240, 477)	(257, 477)	(264, 545)
	Cirrus	Mean $\pm$ SD	308 $\pm$ 134	416 $\pm$ 124	536 $\pm$ 158	459 $\pm$ 134
		Median, IQR	271 (221, 332)	418 (324, 444)	510 (445, 643)	425 (388, 479)
		Range	(164, 652)	(220, 687)	(276, 889)	(258, 752)

Mean  $\pm$  standard deviation, median, inter-quartile range (IQR; first quartile, third quartile), range (minimum, maximum) for the native Spectralis measurements, the Spectralis AIF (rotational reference reset to horizontal acquired image frame) dataset, and the Cirrus measurements

**Table 3** Mean difference (Spectralis minus Cirrus) and standard deviations of the measurements achieved with the two instruments in the different quadrants and global

Group	Quadrant	Differences ( $\mu\text{m}$ )		Correlation coefficients ( $R^2$ )	
		Spectralis - Cirrus	Spectralis AIF - Cirrus	Spectralis ~ Cirrus	Spectralis AIF ~ Cirrus
Overall	Temporal	-28 $\pm$ 83 ( $p < 0.05$ )	-28 $\pm$ 83 ( $p < 0.05$ )	0.892 ( $p < 0.001$ )	0.897 ( $p < 0.001$ )
	Superior	-36 $\pm$ 65 ( $p < 0.005$ )	-28 $\pm$ 64 ( $p < 0.05$ )	0.949 ( $p < 0.001$ )	0.946 ( $p < 0.001$ )
	Nasal	-97 $\pm$ 129 ( $p < 0.001$ )	-96 $\pm$ 130 ( $p < 0.001$ )	0.881 ( $p < 0.001$ )	0.878 ( $p < 0.001$ )
	Inferior	-36 $\pm$ 64 ( $p < 0.001$ )	-45 $\pm$ 64 ( $p < 0.001$ )	0.965 ( $p < 0.001$ )	0.967 ( $p < 0.001$ )
	Global	-49 $\pm$ 77 ( $p < 0.001$ )	-49 $\pm$ 77 ( $p < 0.001$ )	0.949 ( $p < 0.001$ )	0.949 ( $p < 0.001$ )
Glaucoma patients	Temporal	-11 $\pm$ 39 ( $p = 0.2015$ )	-11 $\pm$ 37 ( $p = 0.1903$ )	0.76 ( $p < 0.01$ )	0.78 ( $p < 0.01$ )
	Superior	-5 $\pm$ 35 ( $p = 0.5639$ )	-1 $\pm$ 37 ( $p = 0.9448$ )	0.85 ( $p < 0.01$ )	0.84 ( $p < 0.01$ )
	Nasal	-36 $\pm$ 119 ( $p = 0.1881$ )	-35 $\pm$ 119 ( $p = 0.201$ )	0.57 ( $p < 0.01$ )	0.57 ( $p < 0.01$ )
	Inferior	-3 $\pm$ 33 ( $p = 0.6754$ )	-8 $\pm$ 32 ( $p = 0.2697$ )	0.90 ( $p < 0.01$ )	0.91 ( $p < 0.01$ )
	Global	-8 $\pm$ 48 ( $p = 0.4528$ )	-8 $\pm$ 48 ( $p = 0.4528$ )	0.78 ( $p < 0.01$ )	0.78 ( $p < 0.01$ )
Healthy subjects	Temporal	-68 $\pm$ 97 ( $p < 0.01$ )	-68 $\pm$ 97 ( $p < 0.01$ )	0.86 ( $p < 0.01$ )	0.86 ( $p < 0.01$ )
	Superior	-67 $\pm$ 74 ( $p < 0.01$ )	-56 $\pm$ 74 ( $p < 0.01$ )	0.90 ( $p < 0.01$ )	0.89 ( $p < 0.01$ )
	Nasal	-158 $\pm$ 111 ( $p < 0.01$ )	-158 $\pm$ 112 ( $p < 0.01$ )	0.84 ( $p < 0.01$ )	0.83 ( $p < 0.01$ )
	Inferior	-70 $\pm$ 70 ( $p < 0.01$ )	-81 $\pm$ 69 ( $p < 0.01$ )	0.93 ( $p < 0.01$ )	0.94 ( $p < 0.01$ )
	Global	-91 $\pm$ 80 ( $p < 0.01$ )	91 $\pm$ 80 ( $p < 0.01$ )	0.95 ( $p < 0.01$ )	0.95 ( $p < 0.01$ )

SD standard deviation,  $p$  values paired  $t$  tests. Spectralis AIF—rotationally compensated in order to have the acquired image frame as reference

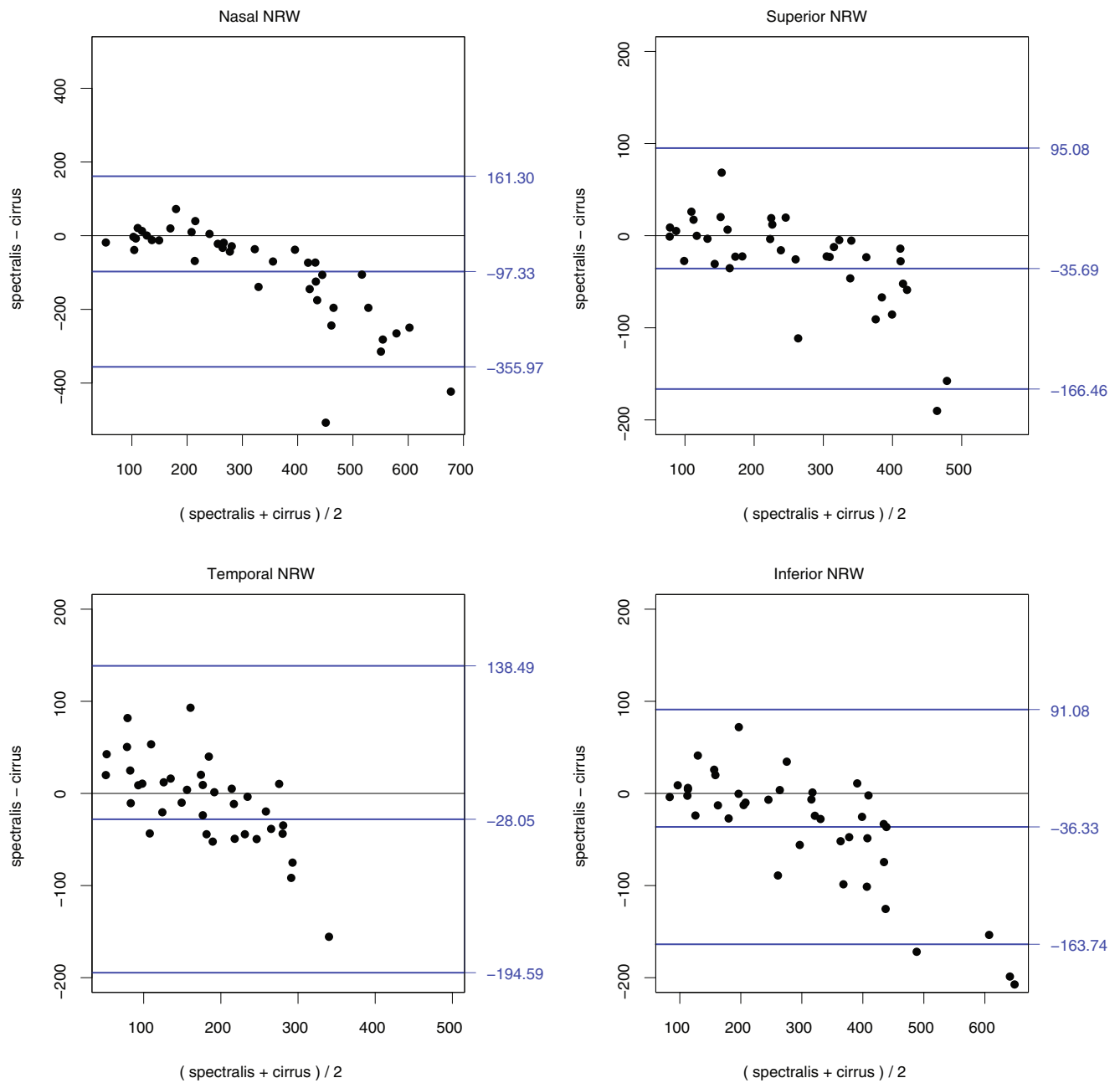


**Fig. 2** Bland-Altman plots of the average neuroretinal rim width measurements of both the Spectralis and Cirrus OCTs for the four quadrants: temporal (tmp), superior (sup), nasal (nas), and inferior (inf).

The middle blue line indicates the mean difference and the upper and the lower lines show the limits of the 95% confidence interval

increasing Cirrus NRW ( $x$ ). Again, both intercept and slope were statistically significant ( $p < 0.001$ ). The residual standard errors of our regression models were  $53.88 \mu\text{m}$  for Cirrus NRW calculated based on Spectralis NRW and  $31.11 \mu\text{m}$  for Spectralis NRW calculated based on Cirrus NRW. The prediction intervals for the mean NRW across patients were  $299 \pm 110 \mu\text{m}$  for the Cirrus NRW and  $249 \pm 68 \mu\text{m}$  for the Spectralis NRW.

**Discrimination capability between glaucoma patients and healthy subjects**

Figure 4 shows continuous plots and boxplots of the NRW of glaucoma patients and healthy subjects acquired with the Spectralis OCT and the Cirrus OCT. Cirrus global NRW differences between healthy subjects and glaucoma patients were on average across all angles  $82 \mu\text{m}$  higher than Spectralis

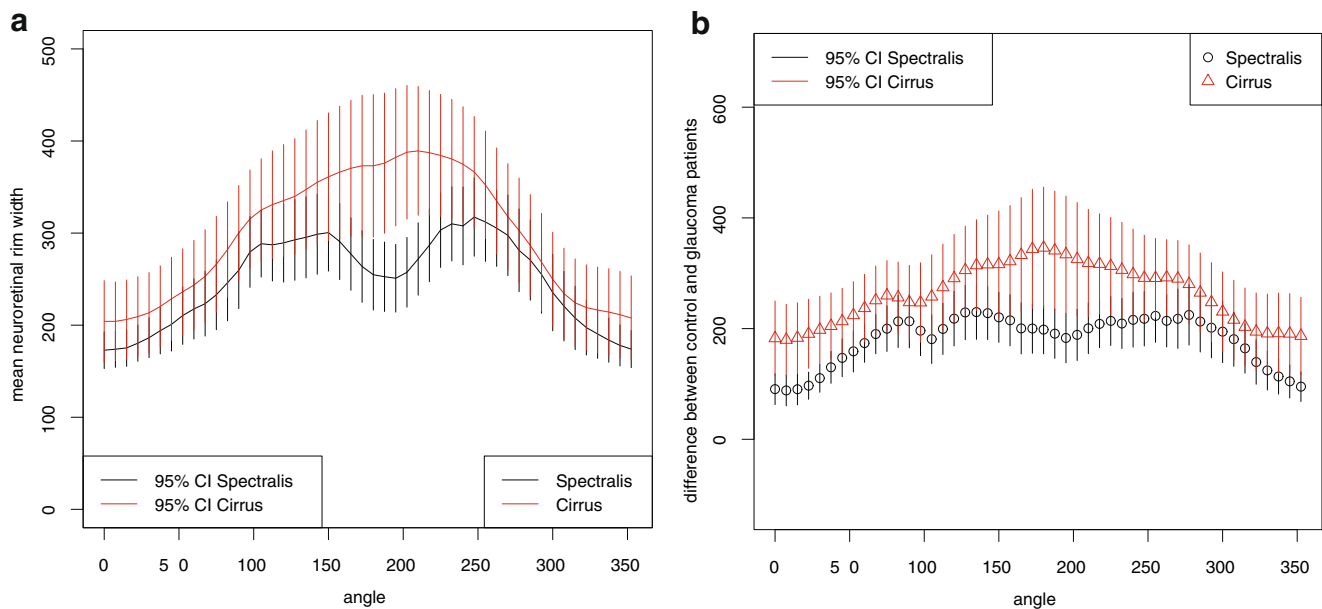


**Fig. 3** **a** Mean neuroretinal rim width across the whole 360° circumference. Values are averaged for each measured angle, depicted separately for the Spectralis (black graph) and the Cirrus OCT (red graph), and plotted along with their 95% confidence intervals. **b** The

global NRW differences ( $p < 0.0001$ , standard error; 4 μm). Figure 3b shows the NRW differences between healthy subjects and glaucoma patients for both devices together with their 95% CI across all different angles. AUROC was 1.0 for the Spectralis and 0.9675 for the Cirrus OCT (see Fig. 5). Online Resource 1 shows the ROC curves and AUROC in the individual quadrants.

### Effect of the rotational alignment discordance on NRW and the results of this analyses

The rotational alignment discordance (anatomic in the Spectralis, image frame in Cirrus) measurements influences NRW and NRW differences only marginally (Table 2 and Table 3). The linear regression term between Spectralis and Spectralis AIF across all 48 angles was  $y = 0.98x + 4.91$  with  $R^2 = 0.9661$  and  $p < 0.001$ .

### Association of covariates

Table 4 shows the correlation coefficients of the NRW with the acquired covariates. Those for CDR, CRW, MD, and PSD were highly statistically significant for both devices, the RNFL thickness was only significant for the Cirrus OCT.

## Discussion

We systematically compared the MRW measurement results of two widely used SD-OCT devices (Carl Zeiss Meditec™

difference in neuroretinal rim width between healthy subjects and the glaucoma patient group, illustrated for the outcomes of Spectralis (black) and Cirrus (red) OCT devices, and plotted for each angle

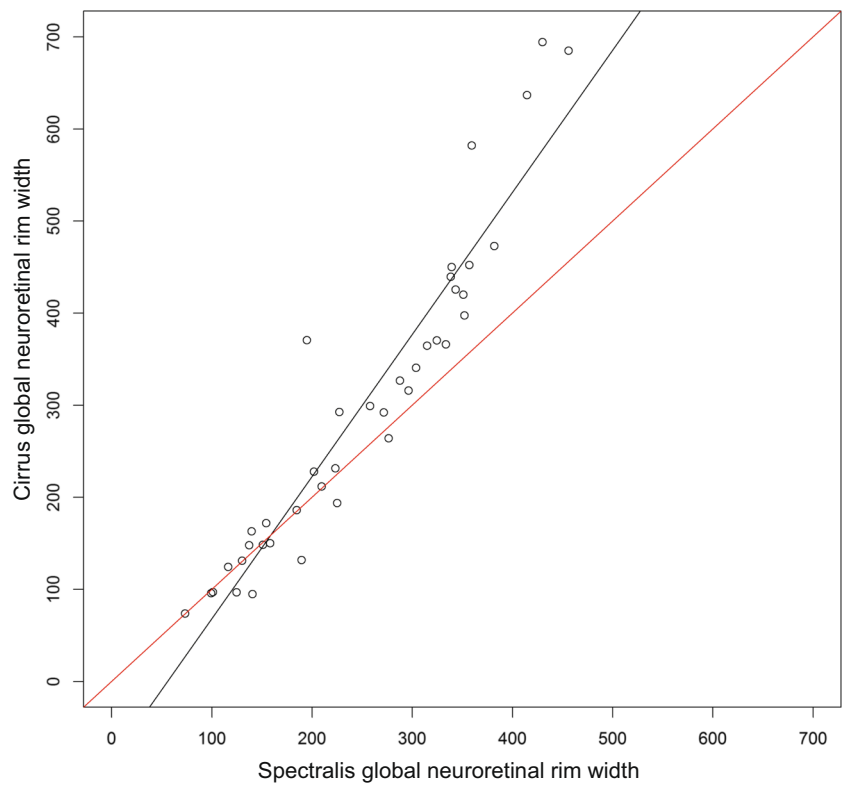
Cirrus HD-OCT® and Heidelberg Engineering™ Spectralis SD-OCT®) for a group of 20 glaucoma patients and a control group of 20 healthy subjects. For healthy subjects, Cirrus mean NRW were markedly higher than Spectralis mean NRW, on average by 91 μm. The difference between devices increased with higher mean NRW values and was especially pronounced for the nasal quadrant (158 μm). On the contrary, for glaucoma patients, NRW was comparable between Cirrus and Spectralis OCT. The causes of the marked differences in healthy subjects may lie in segmentation algorithms, the NRW calculation algorithm itself, and properties concerning scan acquisition and registration.

When comparing healthy subjects and glaucoma patients, our measurements correspond well to results in literature, such as Reis et al. who reported Spectralis OCT-performed NRW measurements of 329 μm for healthy subjects and 176 μm for glaucoma patients [13].

In the current study, Pearson correlations between Spectralis and Cirrus NRW measurements in individual quadrants and for the whole circumference were very strong (all quadrants  $r > 0.8$ , global NRW  $r = 0.949$ ) and of high statistical significance (all  $p < 0.001$ ), for either the native Spectralis dataset or the Spectralis AIF dataset. This seems natural for two devices measuring the same quantity. In their comparison of RNFL thickness measurements with Spectralis OCT and Cirrus OCT, Faghihi et al. reported higher RNFL thickness values with the Spectralis OCT compared with the Cirrus OCT (mean difference was  $4.67 \pm 6.55$  μm,  $p < 0.001$ ) and a strong inter-measurement correlation of  $r = 0.912$  with  $p < 0.001$  [14]. Comparable results were also reported by other



**Fig. 4** Scatter plot of the average neuroretinal rim width measurements using Spectralis and Cirrus optical coherence tomography. The black line gives the result of a linear regression and the red line depicts the values for which the Spectralis measurements are equal the Cirrus measurements



groups [15, 16]. However, to the best of our knowledge, for the NRW this has not yet reported before.

A transformation model between NRW of both devices was rendered, showing that Cirrus shows higher values than

Spectralis for mean measurements being higher than 159  $\mu\text{m}$  (see Fig. 2). Although the correlation of this model was very strong, the applicability is limited because it is based on values of the whole circumference and one may be rather interested

**Fig. 5** Receiver operating characteristics (ROC) curve of Spectralis and Cirrus NRW measurements for the distinction of healthy subjects and glaucoma patients. *AUC* area under the curve

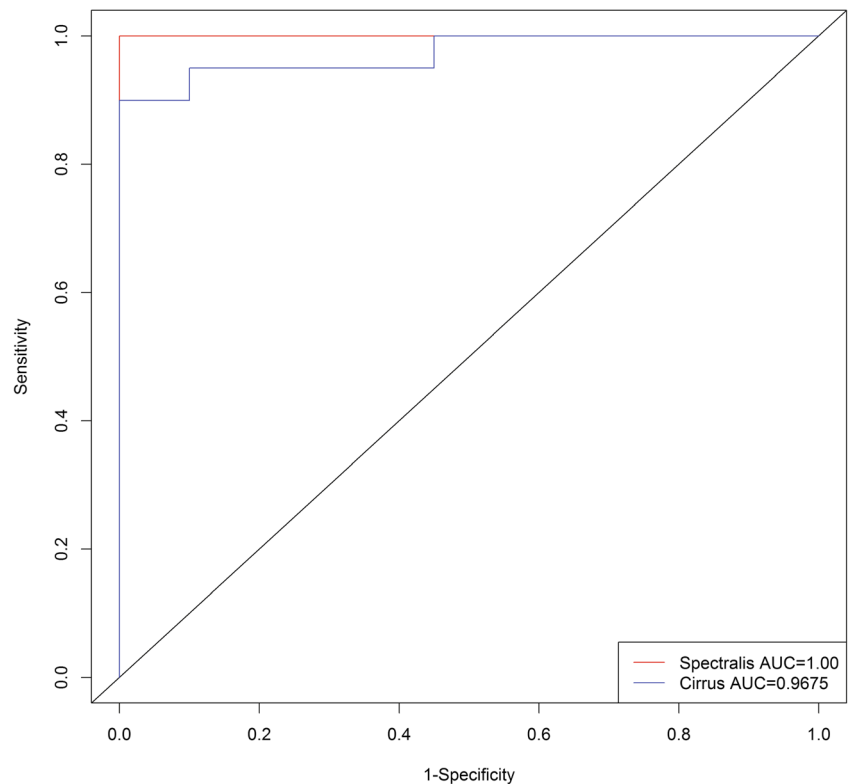


**Table 4** Correlation of the mean neuroretinal rim width (NRW) with different covariates is illustrated for both measurement devices (Spectralis, Cirrus) together with its 95% confidence interval (CI) and *p* value

Covariate	Spectralis mean NRW			Cirrus mean NRW		
	Correlation	95% CI	<i>p</i> value	Correlation	95% CI	<i>p</i> value
BCVA	0.21	(−0.10, 0.49)	0.18	0.14	(−0.18, 0.43)	0.5828
Axial eye length	−0.05	(−0.36, 0.26)	0.74	−0.07	(−0.38, 0.24)	0.6549
Intraocular pressure	0.03	(−0.28, 0.34)	0.8418	<0.01	(−0.31, 0.31)	0.9833
Mean RNFL thickness	0.21	(−0.10, 0.49)	0.1818	0.69	(0.49, 0.83)	<0.001
Cup/disc ratio	−0.92	(−0.96, −0.85)	<0.001	−0.86	(0.72, 0.92)	<0.001
Optic disc diameter	−0.08	(−0.39, 0.26)	0.66	−0.09	(−0.41, 0.24)	0.5828
Calculated rim width	0.90	(0.80, 0.95)	<0.001	0.85	(0.72, 0.92)	<0.001
MD	0.84	(0.72, 0.91)	<0.001	0.72	(0.53, 0.84)	<0.001
PSD	−0.82	(−0.90, −0.68)	<0.001	−0.73	(−0.85, −0.54)	<0.001

BCVA best-corrected visual acuity in Snellen units, MD visual field mean deviation, PSD visual field pattern standard deviation. All correlation tests performed with Pearson's correlation

in values at a specific angle, which may be quite different from the mean across all angles. Furthermore, our models allowed for prediction of NRW across instruments with 53.88  $\mu\text{m}$  (Cirrus NRW calculated based on Spectralis NRW) and 31.11  $\mu\text{m}$  (Spectralis NRW calculated based on Cirrus NRW) residual standard error and prediction intervals of  $299 \pm 110 \mu\text{m}$  for the Cirrus NRW and  $249 \pm 68 \mu\text{m}$  for the Spectralis NRW which will be unacceptable in clinical routine. Furthermore, the given prediction interval is for the mean NRW across patients, and would be even larger for NRW at specific angles.

ROC analysis of NRW revealed both devices and their calculation methods to be excellent classifiers. Given the larger differences between healthy and glaucomatous subjects for the Cirrus as compared with the Spectralis OCT, we might have expected a better discriminatory power for the former. However, this larger difference was counteracted by larger variation for the Cirrus OCT and consequently our ROC analysis did not prove any difference in diagnostic discrimination.

Anyhow, the value of this cross-sectional discrimination capacity continues to be rather academic, as glaucoma diagnosis is multimodal and still largely based on progression detection, and the translational potential of results of case-controlled studies is limited [17]. Furthermore it should be noted that we had included on average moderately advanced glaucoma patients, which improves the diagnostic separation.

The rotational reference difference between devices had only a minor impact on localized NRW values. Our analysis showed that not much effect could be expected solely based on this difference. Only 3.4% of all tested individual NRW values differed by more than 20% between the native value and the computed AIF value. This is less than previously reported by He et al., who found that 10.8% of 222 eyes demonstrated a 20% difference in MRW in their study, which was based on manual delineation [18].

We tested the association of different covariates with the NRW measurements. The CDR as estimated in biomicroscopical examination is a simplified, dimensionally reduced estimation of NRW. Although estimated manually and being prone to subjectivity and human error, it is a morphometric parameter known to increase with the progression of retinal ganglion cell loss in glaucoma. This parameter showed a very strong correlation with NRW acquired with both devices, and performed very similar to the CRW, which takes the ODD into account. This confirms the ODD independence of OCT-based NRW measurements Enders et al. reported recently [5]. Both tested visual field defects, namely the MD and the PSD were also highly correlated with NRW. This is consistent with reports found in literature, such as the study published by Muth et al., where Spectralis OCT global NRW strongly correlated with visual field indices ( $r = 0.68873$  with MD, and  $r = 0.68873$  with PSD, both highly significant) [19].

There are several limitations to our study. A primary issue is the small sample size, but that is in line with other recent approaches. Nevertheless, elaborated differences and correlations mostly show high statistical significance; thus, a generalization is possible. The high ROC values are expected for comparison of moderate to severe glaucoma with healthy subjects and do not indicate an outstanding diagnostic performance. Surprisingly, we found the numerically largest difference in NRW between healthy subjects and glaucoma patients in the nasal quadrant; this was found only in Cirrus OCT. It should be noted however that this quadrant also results in the largest variation in Cirrus OCT and the distribution of values was markedly skewed. The nature of this finding remains unclear, but might be caused by the larger blood vessels together with the specific procedure of segmentation by Cirrus software. This is an exploratory study and our results are preliminary. A solid transformation model needs to be based on the measurements of much bigger patient and control cohorts.

As well as other established functional and morphometric features considered over the course of an often life-long management of glaucoma patients, the NRW will highly likely exhibit its true diagnostic potential when assessed longitudinally. NRW may be used not only in ophthalmological situations, but also others, such as cases with increased intracranial pressure; thus, detailed knowledge about the way this parameter is measured and how measurements differ between devices is quite valuable [20]. We analyze the results of this rather novel objective morphological parameter, as measured by two different devices, which apply considerably differing approaches for its determination. Differences between both devices were much lower and statistically not significant for glaucoma patients, but markedly higher and statistically significant for healthy patients and the whole cohort. It may thus be recommended to compare Spectralis and Cirrus NRW measurements very cautiously and if so then only in patients with morphologically manifest glaucoma. For detailed morphological progression analysis, our results suggest the continuous usage of the same device.

**Funding Information** Open access funding provided by Medical University of Vienna.

### Compliance with ethical standards

**Conflict of interest** The authors declare that they have no conflict of interest.

**Ethical approval** All procedures performed in studies involving human participants were in accordance with the ethical standards of the institutional and/or national research committee and with the 1964 Helsinki Declaration and its later amendments or comparable ethical standards.

**Informed consent** Informed consent was obtained from all individual participants included in the study.

**Open Access** This article is distributed under the terms of the Creative Commons Attribution 4.0 International License (<http://creativecommons.org/licenses/by/4.0/>), which permits unrestricted use, distribution, and reproduction in any medium, provided you give appropriate credit to the original author(s) and the source, provide a link to the Creative Commons license, and indicate if changes were made.

### References

- Weinreb R, Aung T, Medeiros F (2014) The pathophysiology and treatment of glaucoma. *J Am Med Assoc* 311(18):1901–1911
- Medeiros FA, Zangwill LM, Bowd C, Mansouri K, Weinreb RN (2012) The structure and function relationship in glaucoma: implications for detection of progression and measurement of rates of change. *Investig Ophthalmol Vis Sci* 53(11):6939–6946
- Patel NB, Sullivan-Mee M, Harwerth RS (2014) The relationship between retinal nerve fiber layer thickness and optic nerve head neuroretinal rim tissue in glaucoma. *Invest Ophthalmol Vis Sci* 55(10):6802–6816
- van der Schoot J, Vermeer KA, de Boer JF, Lemij HG (2012) The effect of glaucoma on the optical attenuation coefficient of the

- retinal nerve fiber layer in spectral domain optical coherence tomography images. *Invest Ophthalmol Vis Sci* 53(4):2424–2430
- Enders P, Adler W, Schaub F, Hermann MM, Dietlein T, Cursiefen C et al (2016) Novel Bruch's membrane opening minimum rim area equalizes disc size dependency and offers high diagnostic power for glaucoma. *Invest Ophthalmol Vis Sci* 57(15):6596
- Mizumoto K, Goshio M, Zako M (2014) Correlation between optic nerve head structural parameters and glaucomatous visual field indices. *Clin Ophthalmol* 8:1203–1208
- Chauhan BC, O'Leary N, Almobarak FA, Reis ASC, Yang H, Sharpe GP et al (2013) Enhanced detection of open-angle glaucoma with an anatomically accurate optical coherence tomography-derived neuroretinal rim parameter. *Ophthalmology*. 120(3):535–543
- Gracitelli CPB, Abe RY, Medeiros F a. (2015) Spectral-domain optical coherence tomography for glaucoma diagnosis. *Open Ophthalmol J* 9:68–77
- Gardiner SK, Ren R, Yang H, Fortune B, Burgoyne CF, Demirel S (2014) A method to estimate the amount of neuroretinal rim tissue in glaucoma: comparison with current methods for measuring rim area. *Am J Ophthalmol* 157(3):540–549
- Gmeiner JMD, Schrems WA, Mardin CY, Laemmer R, Kruse FE, Schrems-Hoesl LM (2016) Comparison of Bruch's membrane opening minimum rim width and peripapillary retinal nerve fiber layer thickness in early glaucoma assessment. *Invest Ophthalmol Vis Sci* 57:OCT575–OCT584
- Everett MJ, Oakley JD (2015) Automated analysis of the optic nerve head: measurements, methods and representations. <https://www.google.com/patents/US9101293>. Accessed 24 Dec 2018
- R Core Team (2017) R: a language and environment for statistical computing. R Foundation for Statistical Computing, Vienna, Austria. <https://www.r-project.org/>. Accessed 24 Dec 2018
- Reis ASC, Zangalli CES, Abe RY, Silva AL, Vianna JR, Vasconcellos JPC et al (2017) Intra- and interobserver reproducibility of Bruch's membrane opening minimum rim width measurements with spectral domain optical coherence tomography. *Acta Ophthalmol* 95(7):e548–e555
- Faghihi H, Hajizadeh F, Hashemi H, Khabazkhoob M (2014) Agreement of two different spectral domain optical coherence tomography instruments for retinal nerve fiber layer measurements. *J Ophthalmic Vis Res* 9(1):31–37
- Patel NB, Wheat JL, Rodriguez A, Tran V, Harwerth RS (2012) Agreement between retinal nerve fiber layer measures from Spectralis and Cirrus spectral domain OCT. *Optom Vis Sci* 89(5):E652–E666
- Seibold LK, Mandava N, Kahook MY (2010) Comparison of retinal nerve fiber layer thickness in normal eyes using time-domain and spectral-domain optical coherence tomography. *Am J Ophthalmol* 150(6):807–814
- Medeiros FA, Ng D, Zangwill LM, Sample PA, Bowd C, Weinreb RN (2007) The effects of study design and spectrum bias on the evaluation of diagnostic accuracy of confocal scanning laser ophthalmoscopy in glaucoma. *Invest Ophthalmol Vis Sci* 48(1):214–222
- He L, Ren R, Yang H, Hardin C, Reyes L, Reynaud J et al (2014) Anatomic vs. acquired image frame discordance in spectral domain optical coherence tomography minimum rim measurements. *PLoS One* 9(3):15–17
- Muth DR, Himeiß CW (2015) Structure–function relationship between Bruch's membrane opening–based optic nerve head parameters and visual field defects in glaucoma. *Invest Ophthalmol Vis Sci* 56(5):3320
- Qu Y, Wang YX, Xu L, Zhang L, Zhang J, Zhang J et al (2011) Glaucoma-like optic neuropathy in patients with intracranial tumours. *Acta Ophthalmol* 89(5):428–433

**Publisher's note** Springer Nature remains neutral with regard to jurisdictional claims in published maps and institutional affiliations.